Automatic X-ray Stress Measurement System for Cold-rolled Fillet of Solid-type Crankshafts

Dr. Mariko MATSUDA*1 · Hitomi ADACHI*1 · Tatsuhiko KABUTOMORI*2 · Dr. Hiroyuki TAKAMATSU*3
Dr. Toshihiko SASAKI*4

*1 Engineering Department, Steel Casting & Forging Unit, Advanced Materials Business
*2 Production Department, Steel Casting & Forging Plant, Steel Casting & Forging Unit, Advanced Materials Business
*3 Digital Innovation Technology Center, Technical Development Group
*4 Kanazawa University

Abstract

In recent years, attention has been being paid to global environmental problems, and even higher fatigue strength is required for crankshafts used in medium-speed diesel engines for onshore power generation. Surface treatment technology is drawing attention as one of the means to achieve this. In any of the surface treatment technologies, however, a tensile residual stress, which causes a decrease in fatigue strength, occurs at the boundary between the surface treated part and the untreated part, and it is necessary to understand the residual stress distribution around the surface treated part. This paper describes the evaluation of the influence of the macro-segregation peculiar to large, forged steel, and the X-ray incident angle and incident angle setting error, generated during fillet measurement, on the accuracy of X-ray stress measurement by the cos α method. Improvement measures are also described. In addition, the effectiveness of a system that can automatically and high-speed measure the residual stress in the cold rolled fillet has been demonstrated.

Introduction

Recently, the efforts to address global environmental problems have become more active, and reducing greenhouse gas emissions has become a major proposition for medium-speed diesel engines used in onshore power generation. To increase the efficiency and output of engines, crankshafts, which are the main components of engines, are also required to have higher strength and higher fatigue strength than ever before.

Kobe Steel has achieved high fatigue strength by high cleanliness, i.e., reducing the non-metallic inclusions that are inherent in the steel forgings of crankshafts for medium-speed diesel engines,[1] and has been working on further increasing the strength of the materials. However, as it has become clear from general high-strength steel, there are concerns about gigacycle fatigue[2] in high-strength materials exceeding 1,200 MPa, and it is becoming clear that an improvement in fatigue strength cannot be expected to match the increase in production cost.

Hence, surface treatment technology is attracting attention for its potential of further increasing the fatigue strength.[3), 4] Kobe Steel has been developing cold rolling technology for a long time. Cold rolling results in a greater surface treatment depth than other surface treatments and is applicable to large crankshafts.[5] Any surface treatment technology including, but not limited to, cold rolling, suffers from a problem with tensile residual stress caused at the boundary between the surface treated part and the untreated part when compressive residual stress is imparted to the surface treated part. It has been known that compressive residual stress generally improves fatigue strength, while tensile residual stress decreases it.[6] Therefore, when designing a component to be surface treated, it is important to understand the residual stress distribution around the surface treated part.

One of the non-destructive technologies for measuring residual stress is X-ray stress measurement. The conventional X-ray stress measurement based on the $\sin^2\psi$ method,[7] however, involves the use of large apparatuses, each requiring a large space for measurement, making it difficult to perform measurement on narrow parts such as the fillets of crankshafts. In response to this situation, a small portable X-ray stress measurement apparatus based on the $\cos\alpha$ method has become commercially available recently.[8), 9] This apparatus enables simple residual stress measurement in a factory even for crankshaft fillets. However, it has not been long since the use of this apparatus for general purposes began to spread and it reached its current degree of use, and there are still few studies measuring practical materials, compared with the $\sin^2\psi$ method. Therefore, when applying it to the actual crankshafts, which are large, forged steel products, it has been necessary to confirm the validity of the technique.

Also, in the case of X-ray stress measurement based on the $\cos\alpha$ method, the measurement accuracy is known to decrease with a decreasing X-ray incident angle,[10] which is recommended to be around 35°. In the case of crankshafts for medium-speed diesel engines, their size is relatively small among large, forged steel products, and even if X-ray stress measurement is performed with a small

apparatus based on the cos α method, the incident angle at the time of fillet measurement may have to be 20° or lower. In addition, the dimensional tolerances of the actual products make it difficult to accurately grasp the X-ray incident angle for fillets with concave surfaces. Therefore, an error may occur between the input incident angle for stress analysis and the actual incident angle. This has made it necessary to verify the influence that the X-ray incident angle and incident angle error in the cos α method have on measurement accuracy. Furthermore, when measuring narrow parts such as the fillet of a crankshaft, it is an extremely complicated task to irradiate the measurement spot with X-ray under appropriate measurement conditions without making the apparatus come in contact with the measurement target. Thus, automating the X-ray measurement of fillets has been a challenge for practical application.

It is against this backdrop that Kobe Steel studied the validity of the X-ray stress measurement based on the cos α method for low alloy steel with a bainite structure, a typical material, with the aim of applying the measurement to the large, forged steel parts used for the crankshafts of medium-speed diesel engines.[11] Also studied was the influence on the accuracy of X-ray stress measurement of an error occurring between the input incident angle for X-ray stress analysis and the actual incident angle.[12] Furthermore, an automatic X-ray stress measurement system has been developed for the measurement of the fillets of crankshafts. The use of this measurement system has been confirmed to enable the simple measurement of a cold-rolled crankshaft fillet with high accuracy. This paper reports on the results of these studies.

1. Overview of X-ray stress measurement technology based on cos α method

X-ray stress measurement has been studied for a long time, and in it, a technique called the $\sin^2\psi$ method has hitherto been common.[13] In recent years, attention has been focused on measurement by the cos α method using a two-dimensional detector. The X-ray stress measurement principle by the cos α method was first proposed by Taira et al.[14] in 1978, using a photographic film as a detector.

After that, an imaging plate (hereinafter referred to as "IP") appeared in the 1980s, and Yoshioka et al.[15] studied the cos α method using IP as a detector. The size of pixels on the IP was usually a little large, 100 μm, and the pixels were arranged in a grid pattern. Therefore, the application of the cos α method required a high accuracy conversion into X-ray diffraction intensity profiles on a polar coordinate system. In addition, data processing technology with 1/10 pixel or smaller was required for practical stress measurement accuracy. Furthermore, accuracy in determining the center position of the diffraction ring and the smoothing of the image were also important factors.

After 1994, Sasaki et al. solved these series of problems and established the X-ray stress measurement system based on the cos α method using IP.[10] In addition, validity was shown for triaxial stress,[16] macro / micro stress,[17] and the case where the crystal grain is coarse,[18] which had been the problems of X-ray stress measurement. However, the X-ray exposure section and the IP reading section were separated, making the workability generally low and inhibiting widespread use.

In 2009, at JST's new technology briefing session, Sasaki called for the instrumentation of the technology. Taking this as an opportunity, since 2012 several companies have commercialized integrated machines and the like, dedicated to the cos α method one after another. Since the cos α method allows stress measurement by a single X-ray irradiation, the apparatus is smaller, and the space required for the measurement is smaller than that required for the $\sin^2\psi$ method. Furthermore, the advantage of a short measurement time has been demonstrated, and it is now beginning to spread widely.

The cos α method is a technique for obtaining a 360° diffraction ring from a single X-ray irradiation with a two-dimensional detector and calculating stress from the change in the two-dimensional diffraction ring due to the strain of the sample. **Fig. 1** shows the definition of X-ray optics for acquiring a diffraction ring by the cos α method. Here, ψ_0 represents the X-ray incident angle, and 2η represents the angle between the incident X-ray and the diffracted X-ray. The circumference angle α of the diffraction ring in the figure is the angle seen

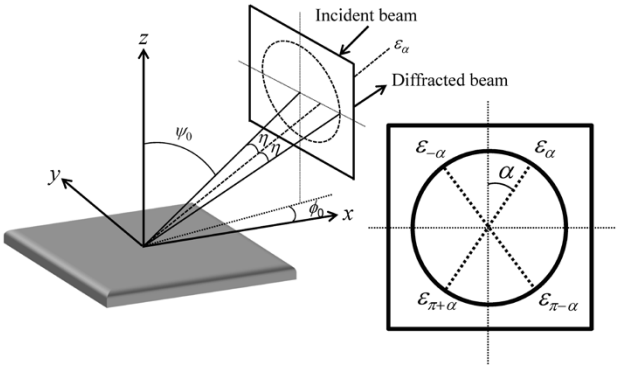

Fig. 1 X-ray optics used for cos α method

from the X-ray tube side. When the X-ray strains whose circumferential angles are α, $-\alpha$, $\pi+\alpha$, and $\pi-\alpha$ are defined to be ε_{α}, $\varepsilon_{-\alpha}$, $\varepsilon_{\pi+\alpha}$, and $\varepsilon_{\pi-\alpha}$, respectively, the parameter a_1 is defined from these strains and is expressed by the following equation.

$$a_1 = \frac{1}{2}\{(\varepsilon_{\alpha}-\varepsilon_{\pi+\alpha})+(\varepsilon_{-\alpha}-\varepsilon_{\pi-\alpha})\} \quad \cdots\cdots\cdots\cdots (1)$$

Assuming a plane stress state and angle η being constant, the following equation holds for the relationship between the stress σ_x in the x direction at the X-ray irradiation point and a_1.

$$a_1 = -\frac{1+\nu}{E}\sin 2\eta \sin 2\psi_0 \cos\alpha \cdot \sigma_x \quad \cdots\cdots\cdots\cdots (2)$$

Here, E and ν represent the X-ray Young's modulus and Poisson's ratio of the sample, respectively. From Eq. (2), a linear relationship holds for $\cos\alpha$ and a_1 ($\cos\alpha$ diagram), and, using the slope of that line, σ_x can be calculated by the following equation.

$$\sigma_x = -\frac{E}{1+\nu}\frac{1}{\sin 2\eta \sin 2\psi_0}\left[\frac{\partial a_1}{\partial \cos\alpha}\right] \quad \cdots\cdots\cdots\cdots (3)$$

The above procedure enables the calculation of stress from the changes in the diffraction ring acquired by a two-dimensional detector.

2. Validity of X-ray stress measurement based on cos α method for crankshaft material of large, forged steel products[11)]

A typical material applied to the crankshafts of medium-speed diesel engines is CrMo-type low alloy steel with a bainite structure. **Table 1** shows the range of content ratio for each chemical composition. In the production of large, forged steel products such as crankshafts for diesel engines, it is difficult to completely avoid macro segregation that occurs in the solidification process of steel ingot. Hence, an evaluation has been conducted on the influence that the high or low macro segregation has on the accuracy of X-ray stress measurement by the $\cos\alpha$ method.

Even if X-ray stress measurement is performed on an actual component, it is difficult to verify the measurement accuracy without knowing the correct value of the residual stress that actually occurs. Therefore, it was decided to perform an X-ray stress measurement for verification on a test body whose stress is known. In other words, a specimen was cut out from an actual component, and an X-ray stress measurement was performed with the tensile stress applied by a universal tensile testing machine. At this time, the accuracy of the X-ray stress measurement was verified by comparing the stress obtained by the X-ray stress measurement with the nominal stress generated in the parallel portion of the specimen. **Fig. 2** shows the appearance of the testing setup. The specimen was a platelet of L150 × W20 × t3 mm. For specimen collection, micro-observation on the cross-section of the actual component was performed to identify sites with high segregation, and two samples were taken from each of the sites with high segregation and those with low segregation.

Table 2 shows the mechanical properties of each specimen. **Fig. 3** shows the observational results of the structure and grain size of the X-ray irradiation site in the specimen with high segregation, and **Fig. 4** shows similar observational results for specimens with low segregation. The main material

Table 1 Range of chemical composition ratios

(mass %)

	C	Si	Mn	Ni	Cr	Mo
Max.	0.45	0.40	1.20	0.50	2.50	0.35
Min.	0.36	0.15	0.80	0.30	1.50	0.15

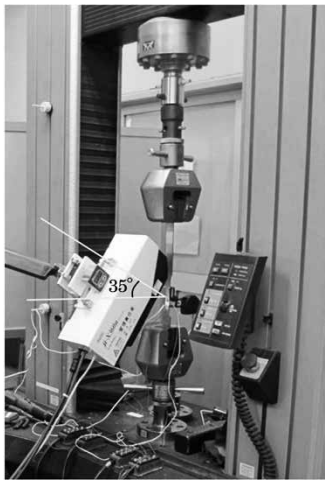

Fig. 2 Tensile test to confirm accuracy of X-ray stress measurement

Table 2 Mechanical properties of specimens

	Tensile strength (MPa)	Proof stress (MPa)
1st. specimen with high segregation	945	813
2nd. specimen with high segregation	987	828
1st. specimen with low segregation	1,035	899
2nd. specimen with low segregation	966	818

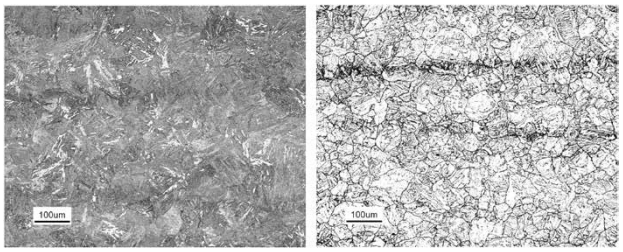

Fig. 3 Microstructures on center of specimen with high segregation

structure of all the specimens was bainite. The average grain size of the specimens with high segregation was 30 to 40 μm, and the average grain size of the specimens with low segregation was 20 to 30 μm, both of which were found to be sufficiently fine for the X-ray stress measurement. However, the specimens with high segregation had a mixed structure in which coarse crystal grains were partially present.

The μ-X360 long range model manufactured by Pulstec Industrial Co., Ltd. was used as the X-ray stress measurement apparatus. In order to exclude the influence of the affected layer that occurs when the specimen is cut out, each specimen was electropolished for a depth of 0.1 mm across a range of 15 × 12.5 mm in the center of the parallel portion. **Fig. 5** shows the appearance of the electropolished area, the X-ray stress measurement position, and their numbers. The X-ray stress measurement was performed at a total of 9 points, 3 × 3 points at a pitch of 3 mm, in the central 9 × 9 mm area in the electropolished part. The Lorentz approximation method, which is the default for μ-X360, was used to determine the peak position of the X-ray diffraction profile. Also, the X-ray elastic constant, $E / (1 + \nu)$ = 175 GPa, recommended by the Society of Materials Science, Japan (JSMS) for ferritic/martensitic steel[19] was used. The X-ray measurement conditions are shown in **Table 3**.

The nominal stress loaded on the specimen by the universal tensile testing machine was set within the elastic stress range, that is, 3 conditions of 1/4, 1/2 and 3/4 of the 0.2% proof stress. Specifically, X-ray stress measurement was performed while gradually increasing the load from the unloaded state. The main purpose of the second specimen was to confirm the reproducibility of the first result. Therefore, with an eye to measurement efficiency, X-ray stress measurement was performed under the condition of only 1/2 of the 0.2% proof stress. The nominal stress generated in the parallel portion of the specimen was calculated from the load cell value of the test machine and the cross-sectional area of the parallel portion of the specimen. At this time, to determine the influence of electropolishing, only the decrease in the thickness of the parallel portion of the specimen was examined. It is considered that stress concentration occurs at the boundary of the electropolished part, and that electropolishing on only one side causes a slight stress difference between the obverse side and reverse side of the specimen. However, preliminary verification has confirmed that their influence is small.

Fig. 6 shows the results of X-ray stress measurement at 9 measurement positions on the first high-segregation specimen and low-segregation specimen. The low-segregation specimen indicates no significant difference in the measured value at the 9 measurement positions for all the applied stresses, whereas the high-segregation specimen is found to have a significant variation in the measured values among the 9 measurement positions. In

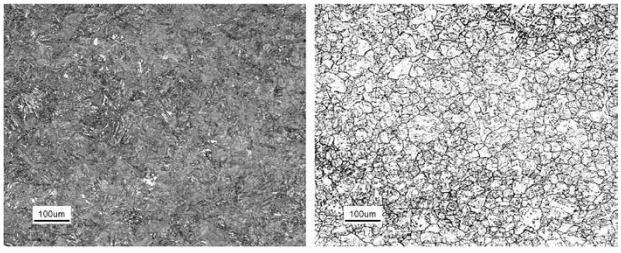

Fig. 4 Microstructures on center of specimen with low segregation

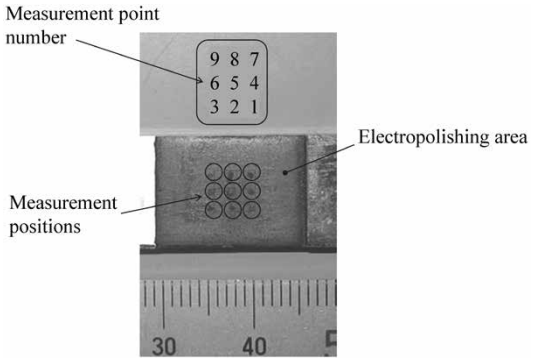

Fig. 5 Appearance of electropolishing area and X-ray measurement positions and their numbers

Table 3 X-ray measurement conditions

Characteristic X-ray	Cr-K_α
Diffraction plane	αFe (211)
Tube voltage	30 kV
Tube current	1 mA
Irradiated area	3 mm^2
Fixed time	30 s
ψ_0 tilt angle	35°
Diffraction angle in stress free	156.4°
Filter	Vanadium foil

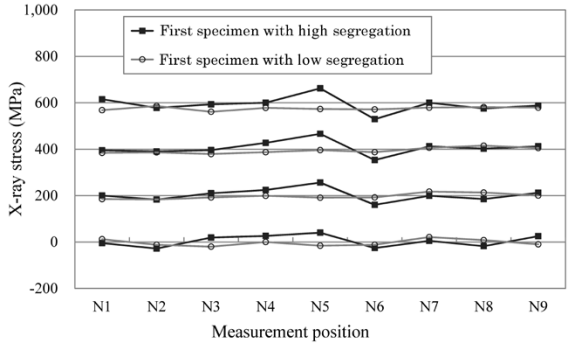

Fig. 6 Results of X-ray measurement at each position of first specimen

addition, the high-segregation specimen shows a large value at the N5 position and a small value at the N6 position, and this tendency is found to be the same regardless of the applied stress of the specimen. This suggests that some conditional difference in the segregated part influences the X-ray stress measurement.

One of the factors that greatly influences the X-ray stress measurement peculiar to the part with segregation is the bias of carbon concentration in the segregated part. If the carbon concentration differs for each X-ray irradiation site, the appearance rate of the second phase such as cementite will be different, which will affect the variation in the stress measurement of the ferrite phase by X-ray. Hence, elemental analysis by FE-SEM was performed by the EDS analyzer on the 9 positions of X-ray stress measurement in the second specimen collected from the high-segregation part. Since the area of the EDS analysis is much smaller than the area of the X-ray irradiation range, elemental analysis was conducted at two different points within the X-ray irradiation range and their average values were used. The results of the elemental analysis are shown in **Fig. 7**. The concentrations of carbon and each alloying element tend to be different for each measurement position. Therefore, the focus has been only on the carbon concentration, which has the greatest influence on the appearance rate of cementite and thus influences the X-ray stress measurement. A comparison was made between the carbon concentration and the X-ray stress measurement value at 9 measurement positions (**Fig. 8**). For the vertical axis in the figure, the difference between the nominal stress and the measured value has been taken. As shown, when the carbon concentration is high, the measured value tends to be higher than the nominal stress, and when the carbon concentration is low, the measured value tends to be lower than the nominal stress. Therefore, the bias of carbon concentration in the segregated part is considered to be one of the causes of the variation in the measurement values of X-ray stress.

Next, **Fig. 9** compares the average values of the X-ray stress, measured at the 9 measurement positions, with the nominal stress in the high-segregation specimen and the low-segregation specimen. Each plot in the figure shows the average value of the measurement at the 9 positions on the respective specimen, and the error range shows the range of maximum and minimum values among the 9 positions. The line in the figure shows the condition where the measured value and the nominal stress match. The average of the values measured at the 9 positions in the first specimen

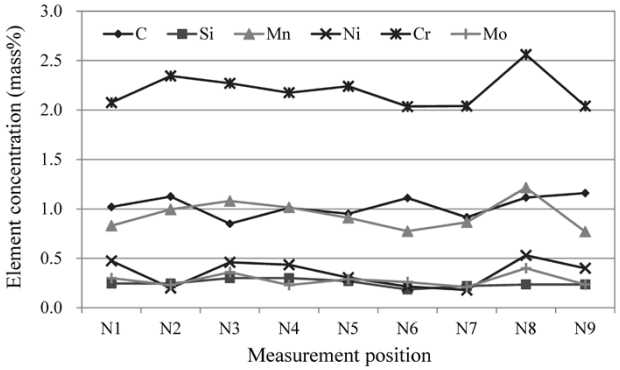

Fig. 7 Element concentration at each position of second specimen with high segregation

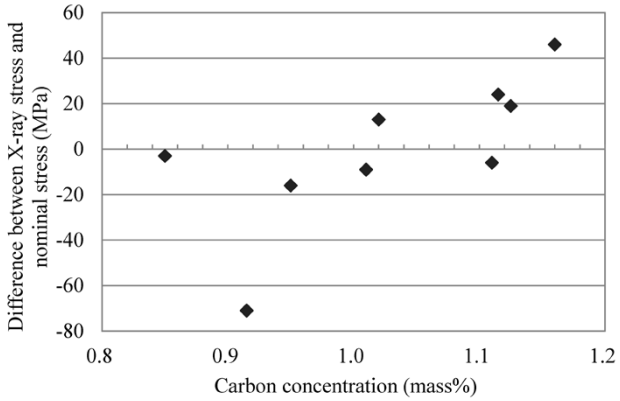

Fig. 8 Relationship between carbon concentration and difference between X-ray stress and nominal stress in second specimen with high segregation

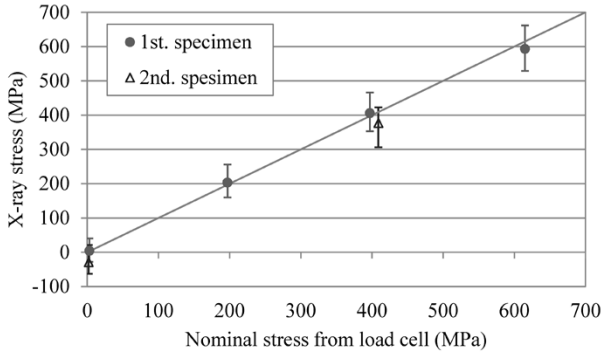

(a) First and second specimens with high segregation

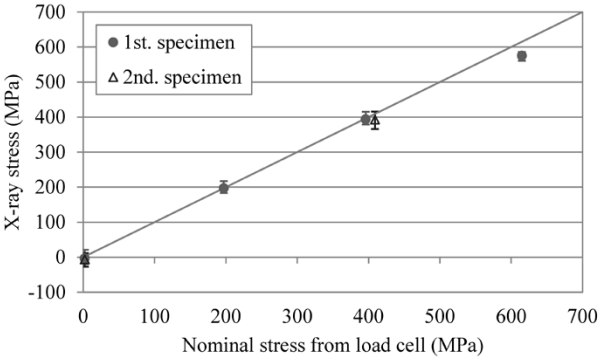

(b) First and second specimens with low segregation

Fig. 9 Comparison between mean value of X-ray stress and nominal stress at 9 measurement points

shows a good agreement between the measured value and the nominal stress for both the high-segregation specimen and low-segregation specimen. On the other hand, in the case of the second specimen, there is a slight difference between the measured value and the nominal stress. Some initial residual stress occurs in the unloaded state, and the slope of the average measured value of the 9 positions is equivalent to that of the first specimen, thus, the initial residual stress is considered to have influenced the measured X-ray stress value.

From these results, in the case of high-segregation specimens, the measured value varies greatly for each X-ray irradiation position, and thus it is difficult to conclude that the measurement with only one point is sufficient for measurement accuracy. Averaging the results of the measurements at 9 positions, however, shows a good agreement between the measured values of X-ray stress and the nominal stress, which is a result similar to the one of low-segregation specimen. Therefore, an adequate number of measurement points (or a sufficient X-ray irradiation area) that can minimize the influence of segregation have been examined. For the 9 measurement positions, all the combinations of adjacent positions when the number of measurement points are 1, 2, 3, 4, 6, and 9 have been considered, and the average value of the X-ray stress measurement at each measurement position has been taken. **Fig.10** compares the high-segregation specimens and low-segregation specimens for the relationship between the number of measurement points and the average X-ray stress value under the condition of 1/4 of the 0.2% proof stress (nominal stress 197 MPa). Both the high-segregation specimen and the low-segregation specimen tended to approach the nominal stress of 197 MPa as the number of measurement points increased. In the case of high-segregation specimens, the error due to the influence of segregation is found to be significantly reduced by 3 points of measurement; and having 4 points of measurement is found to result in the variation of the measured value being at the same level as that of a low-segregation specimen. In the present study, the measurement has been performed under the condition of having the X-ray irradiation area be approximately 3 mm^2, and if the X-ray is irradiated to an area of 4 positions or more, that is, approximately 12 mm^2 or greater, and the measured value is averaged, the influence of segregation can be suppressed to the minimum. In this study, multiple points were measured and averaged. Other means include "using an oscillation method that averages the diffraction ring by swinging the

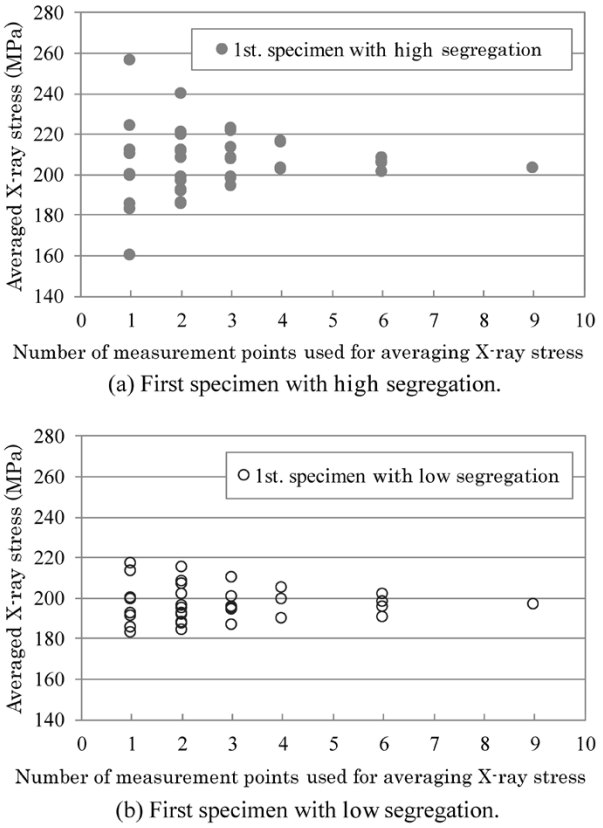

Fig.10 Relationship between number of measurement points used for averaging X-ray stress and averaged X-ray stress in case of nominal stress of 197 MPa

measurement device or the measurement target while irradiating the X-ray," "increasing the X-ray irradiation diameter," and "measuring and averaging the values for the same site with multiple X-ray incident angles." These means are also based on the same idea as this method of increasing the number of crystals from which the diffraction information is retrieved, and all of them are considered to be effective.

3. Influence of X-ray incident angle and incident angle setting error on accuracy of fillet measurement [12)]

It has been shown that the accuracy of the X-ray stress measurement based on the $\cos\alpha$ method decreases at the low incident angle.[10)] However, when the fillet of a crankshaft for a medium-speed diesel engine is measured, the irradiation may have to be done with only a lower incident angle than recommended, depending on the measurement position. In addition, the dimensional tolerances of actual products make it difficult to accurately grasp the X-ray incident angle on the concave curved surface of a fillet. Hence, an investigation has been done to verify the influence of the X-ray incident angle and its setting error on the X-ray stress

measurement accuracy based on the $\cos\alpha$ method.

First, the influence of the X-ray incident angle on the accuracy of X-ray stress measurement was evaluated. Steel pieces were collected from a portion with low segregation in CrMo-based low alloy steel having a bainite structure, equivalent to the one described in Section 2, to prepare a platelet specimen of L150 × W20 × t3 mm. This specimen was subjected to a 4-point bending test, in which X-ray stress measurement was performed by the $\cos\alpha$ method with a tensile (bending) stress loaded. The stress generated in the specimen was calculated from the values of the strain gauge attached to the back surface (concave side) of the specimen. In addition, electropolishing was performed with a depth of 150 μm in a range of 10 × 10 mm at the center of the specimen, and stress measurement was performed at the center of the specimen for the X-ray incident angles of 35°, 15°, 10° and 5°. The detail of the conditions of X-ray stress measurement were roughly the same as those described in Section 2.

Fig.11 shows the influence of the X-ray incident angle on X-ray stress measurement accuracy. The horizontal axis indicates the nominal stress caused by the 4-point bending, the vertical axis indicates the measured value of the X-ray stress, and the solid line in the figure indicates the condition where the nominal stress and the measured value match. For the X-ray incident angles of 10° to 35°, the measured value and the nominal stress are almost the same, but for the incident angle of 5°, the measured value deviates significantly from the nominal stress. In other words, the X-ray incident angle of less than 10° results in an accuracy of X-ray measurement that is insufficient for practical use.

Next, the influence of the setting error of the X-ray incident angle on X-ray stress measurement accuracy has been examined. The stress caused by the $\cos\alpha$ method is calculated by Eq. (3) using the slope of the straight line of the $\cos\alpha$ diagram. Hence, under the conditions where E and ν are constant and η is assumed to be constant, the slope of the straight line has been calculated for each X-ray incident angle of the $\cos\alpha$ diagram, in which σ_x becomes 400 MPa. In addition, theoretical calculation has been conducted for the change in σ_x when the input incident angle for calculating the stress using Eq. (3) deviates by ± 1° and ± 2° from the actual incident angle. **Fig.12** shows the results of the theoretical calculation for the X-ray stress measurement error when the incident angle errors of ± 1° and ± 2° occur for the X-ray incident angle of 5° to 45°. When the incident angle is 35° or higher, the influence of the incident angle error on the measurement error is small. It is shown that the lower the incident angle, the greater the influence of the incident angle error, and when the incident angle is lower than 10°, the influence of the incident angle error becomes huge. It is also shown that, when the incident angle error shifts to the positive side, the influence of the incident angle error becomes smaller than when it shifts to the negative side. It has also been found that the measured stress for the incident angle error shifted to the positive side is smaller than the actual stress, and the measured stress for the incident angle error shifted to the negative side is greater than the actual stress. When residual stress is evaluated, an appropriate judgment must be made as to which shift provides the safer-side evaluation on the basis of the theoretical calculation of this paper.

As a result of the above study, it has been found that the conditions with an X-ray incident angle lower than 10° are inappropriate in terms of measurement accuracy regardless of the influence of either the low incident angle or the incident angle setting error. In other words, for measuring the fillets of crankshafts, it is important to set the measurement conditions so that the X-ray incident angle is 10° or higher.

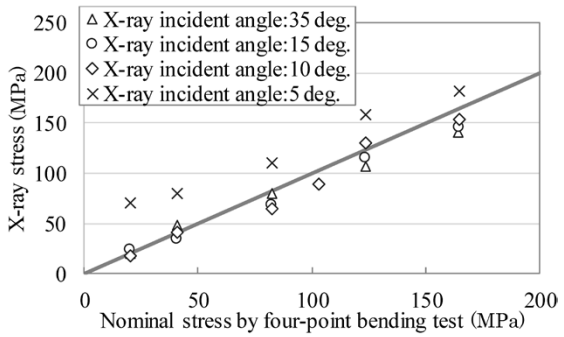

Fig.11 Influence of X-ray incident angle on accuracy of X-ray stress measurement

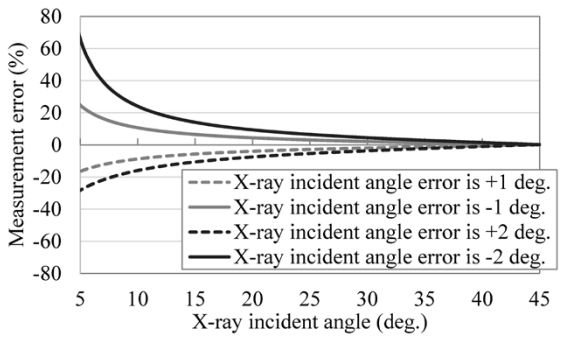

Fig.12 Relationship between X-ray incident angle and measurement error

4. Development of automatic X-ray stress measurement system

On the basis of the results of the above studies, attention must be paid to the following points for the application of the X-ray stress measurement based on the cos α method to the fillets of crankshafts for medium-speed diesel engines.

1) In order to minimize the influence of macro segregation peculiar to large, forged steel products, measurement must be done with multiple points, or with multiple X-ray incident angles and the results must be averaged or with oscillation method.
2) The X-ray incident angle must be set as high as possible (10° or higher), while the incident angle setting error must be kept to the minimum.

There is a limit to the X-ray irradiation distance that can be used for the measurement depending on the measurement position. Therefore, it is necessary to find a measurement condition for setting the X-ray incident angle as high as possible within the constraint range of not hitting the measurement target. However, since the fillets have concave surfaces, the X-ray incident angle and irradiation distance are, respectively, angles and distances relative to the fillet measurement position. Although it is possible to obtain these values by theoretical calculation and determine the optimum setting conditions for the apparatus, it is difficult to actually set the apparatus to the optimum conditions by hand. In addition, since multiple points are measured, it is necessary to set the apparatus multiple times for each measurement point, which requires a huge amount of time and labor.

Hence, Kobe Steel has developed an automatic X-ray measurement system (**Fig.13**). This system includes four types of transfer mechanisms, ① to ④, as shown in Fig.13. Mechanism ① is a rotation mechanism for the crankshaft, and mechanisms ② and ③ are for the transfer in the parallel and vertical directions of the axis of the crankshaft, respectively. Mechanism ④ is a rotation mechanism for adjusting the X-ray incident angle. The transfer mechanisms ② and ③ are used to set the apparatus within the allowable range of X-ray irradiation distance, and the mechanism ④ is used to set the X-ray incident angle as high as possible. This system has a function for judging contact between the measurement target and the apparatus, while a list of the position to be measured and the X-ray measurement conditions can be set in the control unit. This function enables continuous measurement at multiple different positions of the crankshaft fillet without hitting the apparatus on the measurement target, and also supports the oscillation method. For example, by moving only mechanism ① without changing the positional conditions of mechanisms ② to ④, it is possible to perform multiple-point measurement or use the oscillation method while rotating the apparatus in the circumferential direction of the axis of the crankshaft.

Fig.14 shows the results of X-ray stress measurement when this system is applied to a cold-rolled fillet. The horizontal axis represents the angle (fillet angle) of the direction along the fillet with respect to the center of curvature of the fillet, the left vertical axis represents the results of the X-ray stress measurement, and the right vertical axis represents the X-ray incident angle at the time of each measurement points. It has been confirmed that the cold-rolled fillet is imparted with sufficient compressive residual stress for improving fatigue strength.

Fig.14 shows the measurement results of only one position for each fillet angle. If there is concern about the influence of the macro segregation peculiar to large, forged steel products, the measurement accuracy can be improved by measuring multiple points in the circumferential direction of the axis

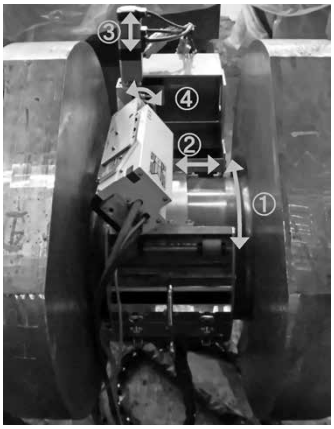

Fig.13 Appearance of developed automatic X-ray measurement

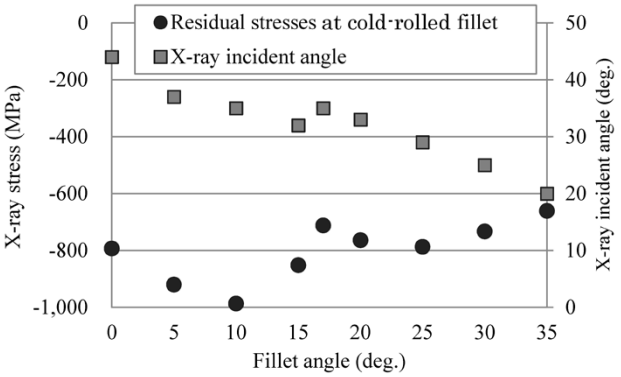

Fig.14 Measurement results of X-ray stresses and X-ray incident angles at cold-rolled fillet of crankshaft

where the cold-rolling condition is considered to be homogeneous, or by using an oscillation method. In manual measurement, there is a concern that the measurement accuracy may decrease due to an error in the incident angle setting. On the other hand, the present system sets the incident angle by the rotation mechanism (④) shown in Fig.13, which suppresses the setting error of the incident angle to the minimum.

From the results of the above studies, this system is considered to be effective in improving the accuracy of X-ray stress measurement based on the $\cos\alpha$ method for crankshaft fillets of medium-speed diesel engines.

Conclusions

This paper has confirmed that, in the case of the CrMo-based low alloy steel, which is a typical material for crankshafts for medium-speed diesel engines, the macro segregation peculiar to large, forged steel products decreases the accuracy of X-ray stress measurement based on the $\cos\alpha$ method. Furthermore, it has been confirmed that multipoint measurement or the oscillation method is effective in suppressing the influence of macro segregation to the minimum.

Also confirmed is the fact that an X-ray incident angle lower than 10° deteriorates the measurement accuracy significantly. When an error occurs between the actual X-ray incident angle and the set incident angle during the stress measurement of a fillet, it has been confirmed by theoretical calculation that the lower the incident angle, the greater the influence of the incident angle error on the stress measurement accuracy.

As a means for solving these accuracy problems, Kobe Steel has developed an automatic X-ray stress measurement system. It has been shown that, when this system is used to measure a cold-rolled crankshaft fillet, highly accurate measurement can easily be performed while suppressing the influence of macro segregation and incident angle setting error to the minimum.

References

1) Ryota Yakura et al. the 27th CIMAC World Congress 2013 in Shanghai. No.422.
2) T. Sakai et al. Journal of The Society of Materials Science, Japan. 2000, Vol.49, No .7, pp.779-785.
3) T. Frondelius. the 28th CIMAC World Congress 2016 in Helsinki. No.180.
4) R. Elvira et al. the 20th International Forgemasters Meeting. 2017.
5) H. Nagasaka et al. R&D Kobe Steel Engineering Reports. 1998, Vol.48, pp.68-71.
6) M. Matsuda et al. Marine Engineering : Journal of the Japan Institution of Marine Engineering. 2020, Vol.55, No.1, pp.3-10.
7) I. C. Noyan et al. Residual Stress Measurement by Diffraction and interpretation. Springer-Verlag, 1987.
8) Y. Maruyama et al. Journal of The Society of Materials Science, Japan. 2015, Vol.64, No.7, pp.560-566.
9) K. Nagao. Journal of the Surface Finishing Society of Japan. 2015, Vol.66, No.12, pp.636-641.
10) T. Sasaki et al. Journal of The Society of Materials Science, Japan. 1995, Vol.44, No.504, pp.1138-1143.
11) M. Matsuda et al. Journal of The Society of Materials Science, Japan. 2019, Vol.68, No.3, pp.285-291.
12) M. Matsuda et al. Japanese Society for Non-destructive Inspection, Proceedings of the 48th Symposium on stress-strain measurement and strength evaluation. 2017, pp.97-100.
13) Japan Society of Materials Science Edition. Revised X-ray stress measurement method. Yokendo Co.,Ltd. 1981.
14) S. Taira et al. Journal of The Society of Materials Science, Japan. 1978, Vol.27, No.294, pp.251-256.
15) Y. Yoshioka et al. Journal of the Japanese Society for Non-Destructive Inspection. 1990, Vol.39, No.8, pp.666-671.
16) T. Sakai et al. Transactions of the Japan Society of Mechanical Engineers (A). 1995, Vol.61, No.590, pp.2288-2295.
17) T. Sakai et al. Transactions of the Japan Society of Mechanical Engineers (A). 1996, Vol.62, No.604, pp.2741-2749.
18) T. Sakai et al. Transactions of the Japan Society of Mechanical Engineers (A). 1997, Vol.63, No.607, pp.533-541.
19) X-ray Material Strength Division Committee, Stress measurement and elasticity subcommittee. Journal of The Society of Materials Science, Japan. 1971, Vol.20, pp.1257-1271.